



# Metabolism of key atmospheric volatile organic compounds by the marine heterotrophic bacterium *Pelagibacter* HTCC1062 (SAR11)

Eric R. Moore , Alec J. Weaver, Edward W. Davis, Stephen J. Giovannoni and Kimberly H. Halsey \*

Department of Microbiology, Oregon State University, 226 Nash Hall, Corvallis, OR, 97331.

## Summary

Plants and phytoplankton are natural sources of the volatile organic compounds (VOCs) acetone and isoprene, which are reactive and can alter atmospheric chemistry. In earlier research we reported that, when co-cultured with a diatom, the marine bacterium *Pelagibacter* (strain HTCC1062; ‘SAR11 clade’) reduced the concentration of compounds tentatively identified as acetone and isoprene. In this study, experiments with *Pelagibacter* monocultures confirmed that these cells are capable of metabolizing acetone and isoprene at rates similar to bacterial communities in seawater and high enough to consume substantial fractions of the total marine acetone and isoprene budgets if extrapolated to global SAR11 populations. Homologues of an acetone/cyclohexanone monooxygenase were identified in the HTCC1062 genome and in the genomes of a wide variety of other abundant marine taxa, and were expressed at substantial levels (c.  $10^{-4}$  of transcripts) across TARA oceans metatranscriptomes from ocean surface samples. The HTCC1062 genome lacks the canonical isoprene degradation pathway, suggesting an unknown alternative biochemical pathway is used by these cells for isoprene uptake. Fosmidomycin, an inhibitor of bacterial isoprenoid biosynthesis, blocked HTCC1062 growth, but the cells were rescued when isoprene was added to the culture, indicating SAR11 cells may be capable of synthesizing isoprenoid compounds from exogenous isoprene.

## Introduction

Acetone ( $C_3H_6O$ ) and isoprene ( $C_5H_8$ ) are abundant volatile organic compounds (VOCs) produced by ocean phytoplankton (Shaw *et al.*, 2003; Colomb *et al.*, 2008; Halsey *et al.*, 2017; Moore *et al.*, 2020). Movement of these VOCs across the sea–air interface initiates complex chemical reactions in the atmosphere that influence climate (Hense *et al.*, 2017). Acetone is a major source of ozone in the troposphere (Müller and Brasseur, 1999; Folkins and Chatfield, 2000) and is sometimes the dominant non-methane atmospheric VOC (Singh *et al.*, 1994). Acetone flux between the ocean and atmosphere is concentration-dependent and variable in direction and magnitude over time and space. Acetone sea–air flux ranges from  $-7$  to  $+8$  Tg yr $^{-1}$ , with the ocean typically acting as a sink for acetone in temperate latitudes and a source in the tropics and sub-tropics (Sinha *et al.*, 2007; Fischer *et al.*, 2012; Beale *et al.*, 2013; Yang *et al.*, 2014). Biological isoprene emissions contribute to about half of the 1000 Tg C global VOC budget (Guenther *et al.*, 2012), are involved in secondary aerosol formation and impact the oxidative capability of the atmosphere (Andreae and Crutzen, 1997; Liakakou *et al.*, 2007). Marine isoprene emissions are estimated at  $0.1$ – $11.6$  Tg C y $^{-1}$  (Palmer and Shaw, 2005; Sinha *et al.*, 2007; Hackenberg *et al.*, 2017), two to three orders of magnitude lower than terrestrial emissions. Discrepancies between measured and modelled flux rates suggest that there is a significant unknown sink for isoprene in the ocean (Palmer and Shaw, 2005; Booge *et al.*, 2017).

Microbial heterotrophic consumption of acetone and isoprene has been hypothesized to account for unexplained variability in sea–air flux rates and VOC budgets. Monthly acetone oxidation rates in the ocean range from  $1$  to  $380$  pmol L $^{-1}$  h $^{-1}$  (Dixon *et al.*, 2013, 2014; Beale *et al.*, 2015). Oxidation rates were highest in the winter or when ‘low nucleic acid’ bacteria, a classification that includes the ubiquitous clade of alphaproteobacteria SAR11, were at their highest cell densities and dominant in the community (Dixon *et al.*, 2014). In soil systems, bacterial acetone metabolism occurs through a variety of biochemical pathways that are typically initiated by an

Received 16 August, 2020; accepted 29 October, 2021. \*For correspondence. E-mail halseyk@science.oregonstate.edu; Tel. 541-737-1831; Fax 541-737-0496. Present address: Bioscience Division, Los Alamos National Laboratory, Los Alamos, NM 87545, USA.

© 2021 The Authors. *Environmental Microbiology* published by Society for Applied Microbiology and John Wiley & Sons Ltd.

This is an open access article under the terms of the Creative Commons Attribution-NonCommercial-NoDerivs License, which permits use and distribution in any medium, provided the original work is properly cited, the use is non-commercial and no modifications or adaptations are made.

acetone monooxygenase enzyme that converts acetone to acetol or methyl acetate (Levine and Krampitz, 1952; Taylor *et al.*, 1980; Kotani *et al.*, 2007). Acetol can be further converted to methylglyoxal, then to pyruvate (Taylor *et al.*, 1980), to formaldehyde and acetic acid (Hartmans and de Bont, 1986), or possibly to formaldehyde and acetaldehyde (Levine and Krampitz, 1952), but this latter pathway has not been verified (Hausinger, 2007). Methyl acetate, the alternative product of the monooxygenase, can be further converted to methanol and acetic acid (Kotani *et al.*, 2007).

Isoprene degrading bacterial communities have been described in estuarine surface water and sediments where heterotrophic consumption of isoprene was sufficient to prevent isoprene emission into the atmosphere (Alvarez *et al.*, 2009; Johnston *et al.*, 2017). A microbial pathway for isoprene metabolism that requires isoprene monooxygenases has been described (van Hylckama Vlieg *et al.*, 2000), and alternative pathways reliant on promiscuous enzymatic reactions have been proposed in cells lacking known isoprene degradation pathways (Patel *et al.*, 1982; Johnston *et al.*, 2017). Although isoprene incorporation from the environment, or isoprene as an intermediate for isoprenoid synthesis, have not been observed, isoprene is commonly present in both soil and marine systems (Dawson *et al.*, 2021), and therefore metabolic strategies reliant on isoprene as a public good could in principle be an effective strategy for cells.

Algal production of VOCs, including acetone and isoprene (Mckay *et al.*, 1996; Shaw *et al.*, 2003; Colomb *et al.*, 2008; Bonsang *et al.*, 2010; Halsey *et al.*, 2017) and their metabolism by heterotrophs, are predicted to impact the net fluxes of these VOCs between the ocean and atmosphere (Alvarez *et al.*, 2009; Dixon *et al.*, 2013; Yang *et al.*, 2014; Booge *et al.*, 2017; Davie-Martin *et al.*, 2020). Complex abiotic photochemistry also impacts sea–air fluxes (Kieber *et al.*, 1990; Mopper *et al.*, 1991; de Bruyn *et al.*, 2011), but these processes cannot fully explain *in situ* observations. Thus, identifying the microbial taxa and metabolisms acting upon these VOCs is needed to explain how and to what extent VOC fluxes are biologically controlled.

*Pelagibacter* is a cultured representative of the SAR11 clade of alphaproteobacteria, the most abundant heterotrophic bacterial family in the ocean (Morris *et al.*, 2002). Recent reports show that *Pelagibacter* metabolizes a wide variety of volatile and methylated compounds, including acetone, for energy generation (Sun *et al.*, 2011; Halsey *et al.*, 2017; Giovannoni *et al.*, 2019; Moore *et al.*, 2020), but evidence for isoprene consumption was less certain (Moore *et al.*, 2020). A role for *Pelagibacter* in controlling sea–air acetone fluxes has been suggested (Dixon *et al.*, 2014), but the rates of consumption by *Pelagibacter* and mechanisms involved

were not known. Here, we demonstrate that dissolved acetone and isoprene are metabolized by *Pelagibacter* strain HTCC1062 and explore the biochemical mechanisms involved. We also show that homologues of the *Pelagibacter* acetone/cyclohexanone monooxygenase comprise about  $10^{-4}$  of transcripts in ocean surface samples.

## Experimental procedures

### Culturing

For all experiments described, *Pelagibacter* strain HTCC1062 (SAR11 group Ia.1) was grown in f/2 artificial seawater medium (Guillard and Ryther, 1962) with the following modifications to support growth of HTCC1062: 0.939 mM KCl, 0.802 mM  $\text{NO}_3^-$ , 1.0 mM  $\text{NH}_4\text{Cl}$ , 0.05 mM glycine, 0.01 mM methionine, 0.078 mM pyruvate, 0.84  $\mu\text{M}$  pantothenate, 0.985  $\mu\text{M}$  4-amino-5-hydroxymethyl-2-methylpyrimidine, 0.3  $\mu\text{M}$  thiamine, 0.002  $\mu\text{M}$  biotin, 0.117  $\mu\text{M}$   $\text{FeCl}_3 \cdot 6\text{H}_2\text{O}$ , 0.009  $\mu\text{M}$   $\text{MnCl}_2 \cdot 4\text{H}_2\text{O}$ , 0.0008  $\mu\text{M}$   $\text{ZnSO}_4 \cdot 7\text{H}_2\text{O}$ , 0.0005  $\mu\text{M}$   $\text{CoCl}_2 \cdot 6\text{H}_2\text{O}$ , 0.0003  $\mu\text{M}$   $\text{Na}_2\text{MoO}_4 \cdot 2\text{H}_2\text{O}$ , 0.001  $\mu\text{M}$   $\text{Na}_2\text{SeO}$ , and 0.001  $\mu\text{M}$   $\text{NiCl}_2 \cdot 6\text{H}_2\text{O}$  (Moore *et al.*, 2020). Cultures were maintained in exponential growth at 16°C, 25  $\mu\text{E}$  light on a 12 h light/dark cycle and shaken gently. Cultures were grown in sterile, acid-washed polycarbonate flasks, or in 10–20 ml glass vials treated with a 5% solution of bovine serum albumin for 8 h, rinsed with Nanopure water then autoclaved. Cell enumerations were conducted by staining 200  $\mu\text{l}$  samples of culture with SYBR Green I for 1–2 h then measured using a Guava flow cytometer.

### Acetone incorporation/oxidation

Incubations of cells with radiolabeled acetone (1,3  $^{14}\text{C}$  acetone, American Radiolabeled Chemicals, St. Louis, MO, USA) were performed to quantify rates of acetone incorporation into biomass ('Incorporation') and oxidation to  $\text{CO}_2$  ('Oxidation') by HTCC1062. This method has been used extensively to study oxidation and assimilation of VOCs (Sun *et al.*, 2011; Halsey *et al.*, 2012). Cultures of HTCC1062 were grown until the late exponential phase. A portion of the culture was heat killed at 55°C for 45 min. Cell enumerations done immediately and 2 days following heat treatment showed no change in cell density compared to cell counts done immediately before heat treatment. 1  $\mu\text{Ci}$  (1  $\mu\text{M}$ ) acetone was spiked into the live and killed cells, activity samples were taken, then 10 ml live cells and killed cells were aliquoted into 20 ml BSA-treated sterile vials and sealed with Teflon faced butyl stoppers. Partitioning of acetone to the headspace of the vial at 16°C was calculated using a dimensionless

Henry's constant (EPA, 2016) to be less than 1% and was therefore considered negligible. Vials were incubated at 16°C in the dark for 0, 2, 5 and 12 h before the incubations were terminated. For measurements of acetone incorporation into biomass, incubations were terminated by adding 1.1 ml of 100% wt./vol. trichloroacetic acid using a syringe. For measurements of combined acetone oxidation and incorporation to biomass, incubations were terminated by adding 0.5 ml 1 M sodium hydroxide, 0.25 ml 0.1 M sodium carbonate and 0.5 ml 1 M barium chloride. Killed cell incubations were terminated after 12 h. Cultures were stored at 4°C for 12 h prior to filtering. The contents of each vial were filtered through 0.1 µm polycarbonate filters and washed three times with either 100% wt./vol. trichloroacetic acid (for 'Incorporation' samples) or 0.2 µm filtered artificial seawater (for total acetone utilization, 'Incorporation + Oxidation' samples). Filters were submerged in Ecoscint scintillation cocktail overnight, sonicated to disrupt and homogenize the contents of the filter, then measured using a scintillation counter (Beckman-Coulter, Brea, CA, USA). Acetone oxidation rates were calculated by subtracting the rate of 'Incorporation' from the total utilization measurement.

#### *Primary growth substrate replacement with acetone*

To test whether acetone could substitute for pyruvate or glycine, which represent two branches of HTCC1062 nutritional requirements (Carini *et al.*, 2012), triplicate 5 ml cultures of HTCC1062 were grown in BSA prepared vials (see above) for each of the following conditions: negative control (growth medium lacking either pyruvate or glycine); positive control [pyruvate (100 µM) and glycine (50 µM) provided]; test conditions (pyruvate or glycine omitted from the medium with acetone supplied at 0.5, 5, 50, 500, or 5000 µM). Cultures were sealed with Teflon-faced butyl septa and incubated at 16°C under gentle shaking with 25 µmol photons m<sup>-2</sup> s<sup>-1</sup> on a 12 h L/D cycle. 200 µl samples were taken with a sterile syringe approximately every other day for cell enumerations.

#### *Inactivation of the isoprenoid biosynthetic pathway*

To test if HTCC1062 could utilize isoprene to meet its isoprenoid requirements for growth, the antibiotic fosmidomycin (Life Technologies, Eugene, OR, USA) was added to HTCC1062 cultures to block the methylerythritol phosphate (MEP) pathway for isoprenoid biosynthesis. The minimum inhibitory concentration for fosmidomycin and HTCC1062 was determined to be 20 µg ml<sup>-1</sup> (data not shown). Quadruplicate 5 ml cultures of HTCC1062 were grown in sealed, BSA-treated glass vials under the following conditions: positive control 1 (No isoprene or fosmidomycin added); positive control

2 [isoprene (10 µM, Sigma-Aldrich, 99.5% analytical standard) with no fosmidomycin]; negative control (no isoprene with fosmidomycin added at 50 µg ml<sup>-1</sup>); test condition [isoprene (10 µM) and fosmidomycin (50 µg ml<sup>-1</sup>) added]. Using a Henry's constant of  $1.3 \times 10^{-4}$  mol m<sup>-3</sup> Pa<sup>-1</sup> (Sander, 2015), the initial concentration of the added isoprene in the aqueous phase after headspace partitioning was calculated to be 2.01 µM at 16°C. Cultures were grown for several weeks and sampled once to twice per week for cell enumerations to determine the peak cell density for each culture.

#### *Gene identification, phylogenetic distribution and environmental abundance*

The acetone monooxygenase and other genes involved in the acetone metabolic pathway previously described in *Gordonia* sp. TY-5 by Kotani *et al.* (2007) were used to search for genes associated with acetone metabolism in HTCC1062. BlastP was used to search the HTCC1062 and 19 other *Pelagibacter* genomes for the published acetone monooxygenase. An acetone monooxygenase was identified (SAR11\_0845) and the functional annotation of the identified gene was validated further by predicting and comparing three-dimensional protein structures to the Protein Data Bank using the program I-TASSER (Yang and Zhang, 2015).

Additionally, the SAR11\_0845 sequence was used in a BlastP search of the nr protein database to identify similar sequences in other taxa. These sequences, plus two validated sequences of phenylacetone (Q47PU3) and cyclohexanone (P12015) monooxygenases from Swiss-Prot, and the protein sequence of the acetone monooxygenase from *Gordonia* sp. TY-5 (A1IHE6) were used to construct a phylogenetic tree comparing the relationships of these genes across taxa using the NGPhylogeny web service (Lemoine *et al.*, 2019). Amino acid sequences were aligned using MAFFT, the alignment was curated with Noisy and a maximum-likelihood phylogenetic tree was constructed with PhyML using 100 bootstrap iterations, and default settings for all programs (Dress *et al.*, 2008; Guindon *et al.*, 2010; Kato and Standley, 2013). iTOL was used to visualize the output tree (Letunic and Bork, 2019), which was re-rooted at the *Gordonia* sp. TY-5 acetone monooxygenase (Kotani *et al.*, 2007).

Blast, implemented by the Ocean Gene Atlas web tool (Villar *et al.*, 2018), was used to search TARA Oceans metagenomes and metatranscriptomes for homologues of the HTCC1062 acetone monooxygenase (SAR11\_0845). The protein sequence of the top HTCC1062 homologue (99% identity) in the Tara oceans dataset, OM-RGC.v2.002142823, was used as a query in a BlastP search against the Tara Oceans metatranscriptome (OM-

RGCv2 + T) database using default settings ( $e^{-10}$  e-value cutoff). The resulting 7546 homologous proteins had 26 689 abundance measures across all samples. Relative abundances of homologues were summed per sample, and summed abundances of surface samples were plotted according to latitude, longitude and season. Data and code for the world map can be found online at <https://github.com/davised/moore-2021-acetone>.

To identify their origin, the 7546 homologous proteins retrieved from metatranscriptomes were aligned using the FFT-NS-i algorithm in MAFFT v7.487 (Katoh and Standley, 2013). Aligned sequences were used as input to FastTree (v2.1.11 SSE3, OpenMP) along with the settings -lg for the Le-Gascuel 2008 amino acid substitution model, -pseudo 1.0 to enable pseudocounts as suggested for highly gapped alignments and -boot 1000 to perform 1000 fast support replicates (Price *et al.*, 2010). The resulting approximate maximum-likelihood tree was midpoint rooted and clades were colour coded according to the taxonomy data supplied for each gene sequence from the Tara database; unlabelled clades either had no taxonomy data supplied or lacked resolution below the domain taxonomic level. The tree figure was generated using the iTOL v5 web interface and then adjusted for publication using Inkscape (Letunic and Bork, 2021).

## Results and discussion

### Acetone metabolism in HTCC1062

Radiolabeled 1,3  $^{14}\text{C}$  acetone was used to measure acetone metabolism in HTCC1062. Cells growing in a defined medium containing pyruvate and glycine, known carbon sources for HTCC1062 (Carini *et al.*, 2012), metabolized acetone at a combined rate of 102 pmol acetone  $10^{10}$  cell $^{-1}$  h $^{-1}$ . Acetone was oxidized to  $\text{CO}_2$  at 85.1 pmol acetone  $10^{10}$  cell $^{-1}$  h $^{-1}$  ( $p = 0.004$ ). Incorporation into biomass was 17.3 pmol acetone  $10^{10}$  cell $^{-1}$  h $^{-1}$  ( $p = 0.008$ ) (Fig. 1). These rates were calculated by considering that both radiolabeled C atoms in the acetone molecule were metabolized; hence metabolism of only a single radiolabeled carbon on each acetone molecule would result in rate values that are twice as fast.

We further tested the ability of HTCC1062 to incorporate acetone into biomass by asking whether acetone could replace the known required HTCC1062 carbon sources, glycine and pyruvate (Carini *et al.*, 2012). Acetone partially replaced glycine as a growth substrate. When acetone was supplied at 500 and 5000  $\mu\text{M}$  in the absence of glycine, HTCC1062 grew approximately two generations more than the negative control ( $p = 0.019$ , 0.048 respectively, Dunnett's test,  $n = 3$ ; Table 1).

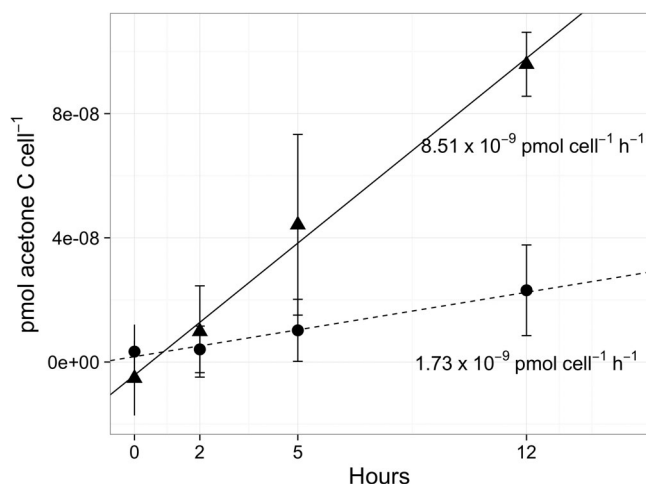


**Fig. 1.** HTCC1062 acetone metabolism. 1,3  $^{14}\text{C}$  acetone was oxidized to  $^{14}\text{CO}_2$  (triangles) at 85.1 pmol acetone  $10^{10}$  cell $^{-1}$  h $^{-1}$  ( $p = 0.004$ ,  $r^2 = 0.99$ ) and incorporated into biomass (circles) at 17.3 pmol acetone  $10^{10}$  cell $^{-1}$  h $^{-1}$  ( $p = 0.008$ ,  $r^2 = 0.98$ ). Lines are linear regressions of oxidized (solid line) and TCA-insoluble radioactive acetone carbon (dashed line). Points are the difference between averages of triplicate samples at each time-point and the average of killed samples; error bars are standard deviations.

HTCC1062 supplied acetone at 0.5, 5 or 50  $\mu\text{M}$  in the absence of glycine did not reach higher maximum cell densities than the negative control ( $p > 0.05$ , Dunnett's test,  $n = 3$ ; Table 1). These results demonstrate that HTCC1062 was capable of incorporating acetone into biomass, providing clarity to the measurements of  $^{14}\text{C}$ -acetone incorporation. The low rate of radiolabeled acetone incorporation shown in Fig. 1 may have been due to the preferential metabolism of glycine (50  $\mu\text{M}$ ) that was supplied to the culture medium in that experiment. Acetone was not able to replace pyruvate as a carbon source at any of the concentrations tested (Table 1).

### Reconstructing metabolic pathways for acetone and cyclohexanone oxidation

Our findings that acetone could be metabolized by HTCC1062 (Fig. 1; Table 1; Moore *et al.*, 2020) prompted us to investigate the mechanisms involved. A gene related to acetone monooxygenase, but annotated as cyclohexanone monooxygenase (SAR11\_0845), was identified in the genome of HTCC1062. Cyclohexanone monooxygenase is part of a gene family that includes acetone monooxygenases and proteins frequently annotated less specifically as NADP/FAD oxidoreductases (Fig. 2). The translated SAR11\_0845 sequence is 32% identical and 53% similar to an acetone monooxygenase described in *Gordonia* sp. TY-5 (Kotani *et al.*, 2007) across 99% of its length. The predicted 3D structure of the SAR11\_0845 protein was structurally similar

**Table 1.** Acetone replaced glycine as a growth substrate when supplied at 500 and 5000  $\mu\text{M}$ .

Treatment	Experiment 1				Experiment 2			
	Glycine		Pyruvate		Glycine		Pyruvate	
	Mean	SD	Mean	SD	Mean	SD	Mean	SD
Negative	$4.93 \times 10^6$	$1.14 \times 10^5$	$5.16 \times 10^5$	$1.24 \times 10^5$	$3.57 \times 10^6$	$6.85 \times 10^5$	$8.91 \times 10^5$	$3.81 \times 10^5$
Positive	$1.23 \times 10^8$	$3.46 \times 10^6$	$8.88 \times 10^7$	$2.88 \times 10^7$	$4.93 \times 10^7$	$3.37 \times 10^7$	$4.93 \times 10^7$	$3.37 \times 10^7$
0.5 $\mu\text{M}$	$5.20 \times 10^6$	$1.51 \times 10^5$	$5.16 \times 10^5$	$8.70 \times 10^4$	–	–	–	–
5.0 $\mu\text{M}$	$5.15 \times 10^6$	$1.04 \times 10^5$	$4.60 \times 10^5$	$6.35 \times 10^4$	–	–	–	–
50 $\mu\text{M}$	$5.39 \times 10^6$	$3.54 \times 10^5$	$5.67 \times 10^5$	$1.30 \times 10^5$	–	–	–	–
500 $\mu\text{M}$	–	–	–	–	<b><math>1.49 \times 10^7</math></b>	$4.99 \times 10^6$	$9.06 \times 10^5$	$2.43 \times 10^5$
5000 $\mu\text{M}$	–	–	–	–	<b><math>1.08 \times 10^7</math></b>	$1.86 \times 10^6$	$1.14 \times 10^6$	$5.18 \times 10^5$

Shown are the mean maximum cell densities of HTCC1062 cultures ( $n = 3$ ) growing on acetone in the absence of glycine or pyruvate. Two separate experiments tested growth on acetone in two ranges of concentration: 0.5–50  $\mu\text{M}$  (Experiment 1) and 500–5000  $\mu\text{M}$  (Experiment 2). Negative control: no glycine or pyruvate supplied and no acetone supplied. Positive control: both pyruvate (100  $\mu\text{M}$ ) and glycine (50  $\mu\text{M}$ ) supplied and no acetone supplied. Final cell densities in experimental cultures that were significantly greater than negative control are shown in bold ( $p < 0.05$ , Dunnett's test).

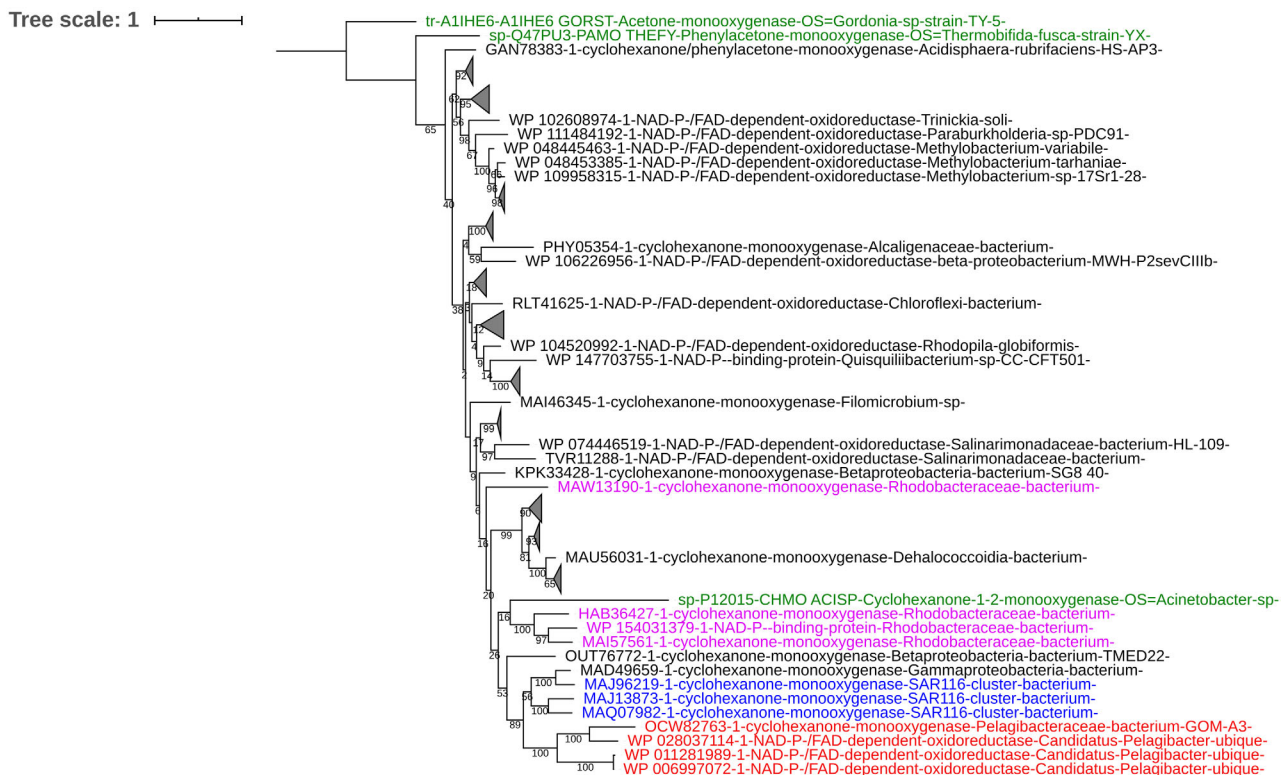


**Fig. 2.** Maximum likelihood phylogenetic tree showing the relationship of the putative SAR11 acetone monooxygenase (SAR11\_0845) and the 100 most similar protein sequences in the nr protein database identified by BlastP. Tree was constructed using 100 bootstrap iterations and re-rooted by the previously described acetone monooxygenase of *Gordonia* strain TY-5 (Kotani *et al.*, 2007) shown in green. Other experimentally validated cyclohexanone and phenylacetone monooxygenases from Swiss-Prot are included and shown in green (Chen *et al.*, 1988; Fraaije *et al.*, 2005). Putative acetone/cyclohexanone monooxygenases are present in abundant marine bacteria including SAR11 (red), SAR116 (blue) and Rhodobacteraceae (violet) (González and Moran, 1997; Rappé and Giovannoni, 2003; Morris *et al.*, 2012).

(TM scores greater than 95%, structural coverage greater than 98%) to cyclohexanone and phenylacetone monooxygenases, enzymes that are commonly multifunctional with a variety of ketone substrates (Chen *et al.*, 1988; Kotani *et al.*, 2007). Acetone monooxygenases catalyse

the conversion of acetone to acetol or methyl acetate (Levine and Krampitz, 1952; Taylor *et al.*, 1980; Kotani *et al.*, 2007), while cyclohexanone monooxygenase oxidizes cyclohexanone to  $\epsilon$ -caprolactone (Donoghue and Trudgill, 1975).

A search of the non-redundant protein database with SAR11\_0845 returned cyclohexanone monooxygenases, acetone monooxygenases and NADP/FAD oxidoreductases that originated from diverse taxa and were about 50% similar with *c.* 98% coverage (Fig. 3). Of particular interest were hits to genes in other bacterial taxa that are abundant in marine epipelagic microbial communities, for example the SAR116 clade, and *Rhodobacteraceae*, the family that includes *Roseobacter* (González and Moran, 1997; Rappé and Giovannoni, 2003; Morris *et al.*, 2012). The topology of the phylogenetic tree shows a close relationship between the HTCC1062 and SAR116 monooxygenases, suggesting that this gene was horizontally transferred among these co-occurring, but evolutionarily distinct organisms.

To study the distribution of SAR11 acetone monooxygenase genes across the SAR11 clade, we used BLAST to search all publicly available SAR11 MAGS, SAGS and genome sequences (Pachiadaki *et al.*, 2019). Acetone monooxygenases were frequently detected in two SAR11 subclades: IB.2, which is found in the surface waters of subtropical seas, and IA.1, which includes strain HTCC1062 and is found at high latitudes (Giovannoni, 2017).

We hypothesize that SAR11\_0845 is a multifunctional enzyme that is active on both acetone and cyclohexanone, and possibly other ketones. A related acetone monooxygenase described in *Gordonia* sp. TY-5 was highly active on a variety of ketones, especially cyclic ketones such as cyclohexanone (Kotani *et al.*, 2007). We previously observed that HTCC1062 metabolized cyclohexanol produced by the diatom *Thalassiosira*

*pseudonana* in co-culture (Moore *et al.*, 2020). The *Pelagibacter* enzyme most likely responsible for cyclohexanol oxidation is an alcohol dehydrogenase [i.e. Fe-Adh (Sun *et al.*, 2011)], which is predicted to produce the product cyclohexanone. The prediction of cyclohexanone monooxygenase activity in SAR11\_0845 fills the first gap in a hypothetical pathway for cyclohexanone oxidation, producing  $\epsilon$ -caprolactam from cyclohexanone (Donoghue and Trudgill, 1975), which could be further metabolized by annotated *Pelagibacter* enzymatic functions, leading to the formation of adipate and feeding downstream beta-oxidation pathways (Donoghue and Trudgill, 1975).

#### Microbial control of acetone sea-air emissions

This study points to a number of abundant marine bacteria that encode acetone/cyclohexanone monooxygenases and could exert control on acetone emissions to the atmosphere (Sinha *et al.*, 2007; Fischer *et al.*, 2012; Beale *et al.*, 2013; Yang *et al.*, 2014). Acetone oxidation rates in coastal waters of the UK ranged from 1 to 42 pmol L<sup>-1</sup> h<sup>-1</sup>, but these rates did not include rates of acetone assimilation (Dixon *et al.*, 2013). Acetone oxidation rates were highest when 'low nucleic acid' bacteria, a classification that includes *Pelagibacter*, were most abundant (Dixon *et al.*, 2014; Yang *et al.*, 2014). Based on the rate of acetone metabolism in *Pelagibacter* cultures (Fig. 1), acetone consumption *in situ* by *Pelagibacter*, at an average concentration of  $2 \times 10^8$  cells L<sup>-1</sup>; (Morris *et al.*, 2002) would be just slightly higher than 1 pmol L<sup>-1</sup> h<sup>-1</sup>. This rate is at the low end of

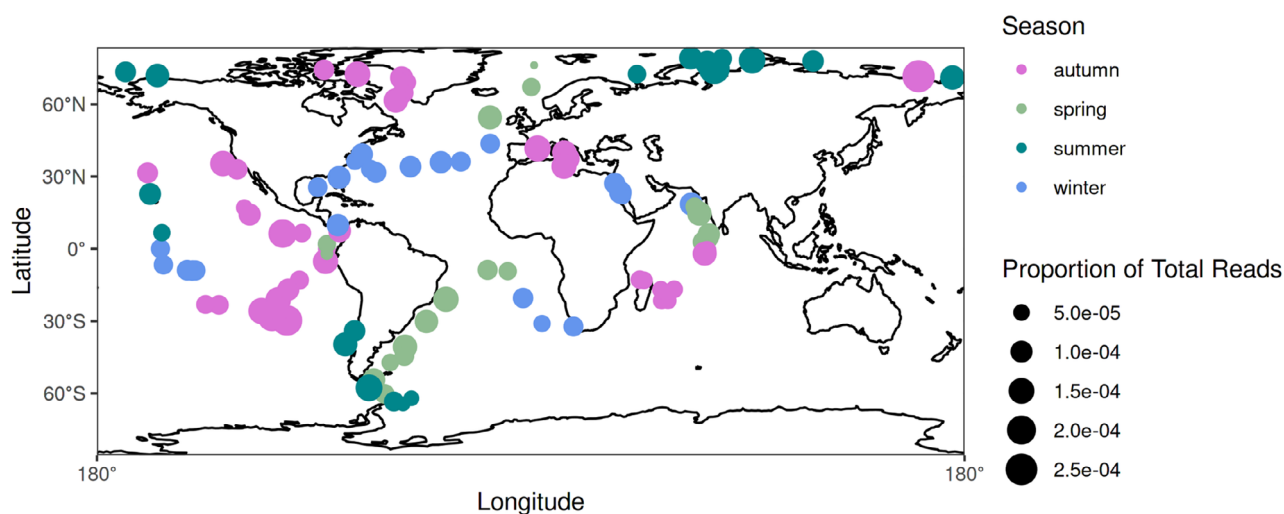


**Fig. 3.** Relative abundances of acetone/cyclohexanone monooxygenases in TARA Oceans meta-transcriptomes from surface samples. The protein sequence of the best hit to the HTCC1062 gene (99% identity) in the TARA oceans dataset, OM-RGC.v2.002142823, was used as a query in a BlastP search against TARA Oceans metatranscriptome database, using default parameters. The phylogenetic distribution of sequences from this analysis is shown in Fig. S1.

**Table 2.** 10  $\mu\text{M}$  isoprene partially rescued the growth of HTCC1062 in the presence of the MEP pathway inhibitor fosmidomycin (Fos).

	No isoprene		10 $\mu\text{M}$ isoprene	
	No Fos.	No Fos.	50 $\mu\text{g ml}^{-1}$ Fos.	50 $\mu\text{g ml}^{-1}$ Fos.
# Cultures with positive growth	4 of 4	4 of 4	0 of 4	3 of 4
Mean final density (cells $\text{ml}^{-1}$ )	$5.01 \times 10^7$	$3.02 \times 10^7$	$9.67 \times 10^4$	$2.18 \times 10^6$
SD	$2.21 \times 10^6$ ( $n = 4$ )	$3.70 \times 10^7$ ( $n = 4$ )	$1.45 \times 10^4$ ( $n = 4$ )	$2.10 \times 10^6$ ( $n = 3$ )
Inoculation density (cells $\text{ml}^{-1}$ )	$1.00 \times 10^5$	$1.00 \times 10^5$	$1.00 \times 10^5$	$1.00 \times 10^5$

HTCC1062 could not grow when the MEP pathway was inhibited by fosmidomycin in the absence of isoprene. Positive growth was defined as 2 or more divisions (cell density  $\geq 4.00 \times 10^5$  cells  $\text{ml}^{-1}$ ) above the starting concentration of the culture ( $1.00 \times 10^5$  cells  $\text{ml}^{-1}$ ).

the oxidation rates measured *in situ* but was derived from only one *Pelagibacter* strain in culture. Further investigations of VOC metabolism by other marine taxa possessing acetone monooxygenases under different environmental conditions will reveal a more comprehensive understanding of microbial VOC cycling and controls on VOC sea–air emissions.

We examined the distribution of acetone monooxygenase transcripts in TARA oceans transcriptome data (Fig. 3) and found that genes related to SAR11 acetone monooxygenases are frequently expressed in surface ocean waters (c.  $0.5\text{--}2.5 \times 10^{-4}$  of all transcripts) at all latitudes (Villar *et al.*, 2018). To examine phylogenetic relationships among the acetone monooxygenase genes retrieved from TARA oceans data, we used FastTree and taxonomy assignments from TARA oceans. SAR11\_0845 homologues were found in a diversity of taxa (Fig. S1).

In the western North Atlantic Ocean, the rates of net acetone production were strongly positive during the annual phytoplankton bloom climax with rates increasing from a mean of  $3.2 \text{ nmol L}^{-1} \text{ h}^{-1}$  in the south to  $37.3 \text{ nmol L}^{-1} \text{ h}^{-1}$  in the north (Davie-Martin *et al.*, 2020). Net acetone production is positively correlated with nanoeukaryotic phytoplankton (Beale *et al.*, 2015; Davie-Martin *et al.*, 2020). Despite biological acetone production outpacing its consumption by heterotrophs, seawater is under-saturated with respect to acetone in the sub-polar North Atlantic and sea–air flux rates are not sufficiently large to account for the low concentration of acetone in seawater (Beale *et al.*, 2015). In contrast, rates of net acetone production were near zero in the summer months when primary production was low, seawater acetone concentrations at their highest (16 nM) (Davie-Martin *et al.*, 2020), and the turnover rate of acetone is low (165 days in the summer compared to 6 days in the winter) (Dixon *et al.*, 2013; Beale *et al.*, 2015).

The complex relationships between acetone in-water concentrations and sea–air flux suggest that the abundance and expression of acetone/cyclohexanone genes shown in Fig. 3 reflect the presence and activity of the biological sources of acetone, as well as its consumption and use as a growth substrate by abundant heterotrophic

bacteria (Fig. 2 and Fig. S1). The identification of SAR11\_0845 homologues in other common marine bacterial clades, including SAR116 and Rhodobacteraceae, suggests the genetic potential for acetone metabolism is not particularly rare, thus large populations of bacteria may fill a niche provided by acetone bioavailability and collectively contribute to acetone turnover. Our findings show that total rates of acetone catabolism by HTCC1062 in axenic culture (Fig. 1) were not as high as the maximum oxidation rates reported in seawater (Beale *et al.*, 2013; Dixon *et al.*, 2014), suggesting additional taxa were likely involved to achieve higher total consumption rates observed in seawater. Furthermore, direct measurements of *in situ* acetone metabolism have been spatially and temporally restricted, thus future investigations that provide greater resolution on the total microbial consumption of acetone *in situ* will clarify the significance of microbial controls on marine acetone flux.

#### Isoprene metabolism

The data we report in this section suggest that HTCC1062 possesses an undescribed biochemical pathway that enables it to use freely diffusing isoprene from the environment to meet isoprenoid biosynthesis requirements. We previously reported that isoprene stimulated ATP production in HTCC1062 (Moore *et al.*, 2020). However, unlike acetone, which supported both energy generation and growth (Fig. 1), isoprene did not support the growth of HTCC1062 in the absence of pyruvate or glycine (data not shown). We next asked whether isoprene could meet the isoprenoid requirements of HTCC1062 under metabolic challenge. Fosmidomycin is an antibiotic that competitively inhibits 1-deoxy-D-xylulose 5-phosphate reductoisomerase (Dxr) in the second step of the MEP isoprenoid synthesis pathway, which is encoded in the HTCC1062 genome (Fig. 4). Growth of HTCC1062 was sensitive to  $50 \mu\text{g ml}^{-1}$  fosmidomycin. Addition of  $10 \mu\text{M}$  isoprene ( $2 \mu\text{M}$  in aqueous phase, see Experimental procedures) rescued HTCC1062 cells in the presence of fosmidomycin (Table 2). These results show that HTCC1062 is able to use isoprene to bypass

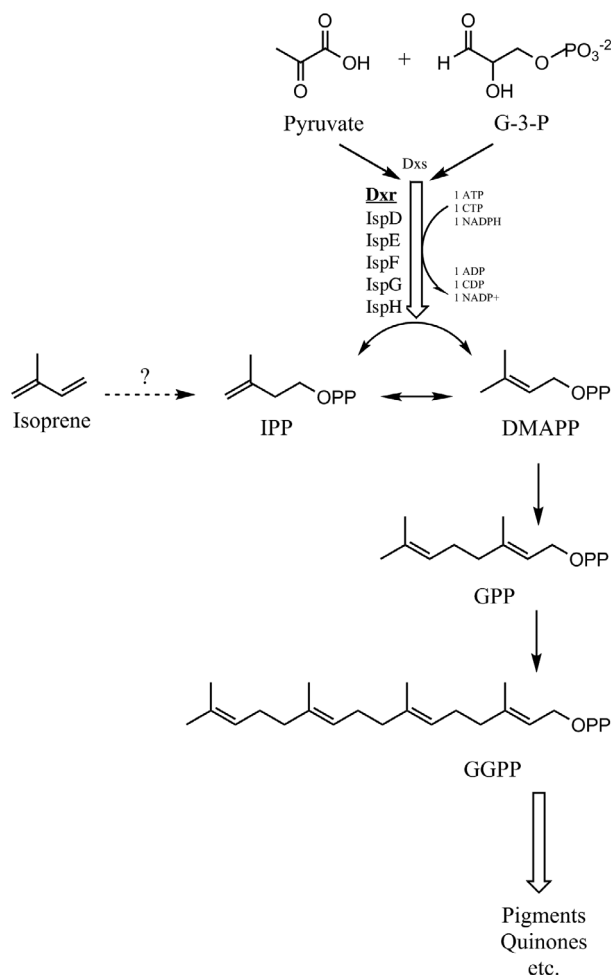


**Fig. 4.** The methyl erythritol phosphate (MEP) pathway for biosynthesis of the isoprenoid precursors isopentenyl pyrophosphate (IPP) and dimethylallyl pyrophosphate (DMAPP) from pyruvate and glyceraldehyde-3-phosphate (G-3-P) in HTCC1062. The second enzyme of this pathway, Dxr is competitively inhibited by the antibiotic fosmidomycin (shown in bold/underline). Isoprene rescued growth of HTCC1062 when this pathway was blocked with fosmidomycin. The dashed line indicates a hypothetical reaction that might allow HTCC1062 to use isoprene as a precursor for IPP and DMAPP. No enzyme is known that catalyses this reaction.

the isoprenoid biosynthetic pathway when it is blocked by fosmidomycin.

Isoprene monooxygenase, the canonical enzyme that initiates isoprene metabolism in Actinobacteria, facilitates its use as a carbon source for growth (van Hylckama Vlieg *et al.*, 2000; Johnston *et al.*, 2017), is absent from the HTCC1062 genome. BLAST searches that used the *Rhodococcus* isoprene monooxygenase as a query failed to detect homologues. Isoprene is not an intermediate in the MEP pathway leading to isoprenoid biosynthesis, and no known pathway exists whereby isoprene can be converted to the key isoprenoid subunits, isopentenyl pyrophosphate (IPP) and dimethylallyl pyrophosphate (DMAPP). The simplest possible route might be terminal

oxidation of isoprene to isopentanol and sequential phosphorylation to form IPP and DMAPP (Fig. 4). No evidence for such a path currently exists, but the global ubiquity of isoprene including in marine environments (McGenity *et al.*, 2018) highlights the need for understanding alternative isoprene metabolism pathways.

Isoprenoids are used for biosynthesis of electron carriers, such as ubiquinone, porphyrin-based compounds, and in HTCC1062, biosynthesis of the pigment retinal, which is a key component of the light-harvesting protein proteorhodopsin. Cells typically rely on small pools of electron carriers, so the demand for isoprenoids in HTCC1062 is likely small but critical, ensuring maintenance of the MEP pathway in the genome, despite evolutionary streamlining (Giovannoni *et al.*, 2005a; Giovannoni *et al.*, 2005b) and the steady availability of isoprene produced by phytoplankton (Mckay *et al.*, 1996; Colomb *et al.*, 2008; Bonsang *et al.*, 2010; McGenity *et al.*, 2018). For organisms like HTCC1062, bypassing the carbon and energy requirements for isoprenoid synthesis, [each isoprenoid subunit requires 6C, 1 ATP, 1 CTP and 1 NADPH; (Zhao *et al.*, 2013)], could facilitate growth in the dilute carbon of the open ocean. However, the energy savings would only be 1 NADPH in our model.

We used cell proteorhodopsin content to estimate a minimum isoprene demand in HTCC1062. A number of different essential compounds found within these cells require isoprenoid precursors, but cell quotas are available for retinal, making it a useful point of reference for evaluating the potential SAR11 cell demand for isoprene. Four isoprene (5 C) molecules are required for biosynthesis of each retinal (20 C) molecule in proteorhodopsin, thus 40 000 isoprene molecules would be required to supply retinal to the 10 000 proteorhodopsin in each HTCC1062 cell (Giovannoni *et al.*, 2005a; Giovannoni *et al.*, 2005b). Assuming the entire standing stock of  $2.4 \times 10^{28}$  SAR11 cells worldwide is capable of using isoprene to fulfil its isoprenoid requirements, and a population turnover rate of  $0.3 \text{ d}^{-1}$  (White *et al.*, 2018), the maximum potential SAR11 contribution to global marine isoprene uptake is  $11.9 \text{ Tg y}^{-1}$ . This value is remarkably similar in magnitude to the entire marine isoprene budget of  $0.1\text{--}11.6 \text{ Tg C y}^{-1}$  (Palmer and Shaw, 2005; Sinha *et al.*, 2007; Hackenberg *et al.*, 2017) but is an underestimate that does not consider other essential isoprenoids, such as quinones or porphyrins, or other taxa or metabolic strategies involved in isoprene degradation. Nevertheless, our data and estimates indicate that the use of isoprene by HTCC1062, and other heterotrophic bacteria that potentially encode canonical isoprene monooxygenase pathways, are of such magnitude that they would likely impact isoprene concentrations and turnover in the ocean. The identification of bacterial isoprene



uptake activity provides an explanation for observed discrepancies between predicted and measured isoprene flux rates to the atmosphere that have implied a previously hidden bacterial sink for isoprene in the ocean.

## Conclusion

We found that *Pelagibacter* strain HTCC1062 (SAR11) metabolizes acetone and isoprene, two VOCs that are produced by phytoplankton and cross into the atmosphere where they are reactive and influence climate. We show that homologues of the protein most likely responsible for acetone oxidation in *Pelagibacter* are widely expressed in ocean surface transcriptomes. We present evidence that *Pelagibacter* possesses an undescribed biochemical pathway that enables it to use freely diffusing isoprene from the environment to meet isoprenoid biosynthesis requirements. This suggests that further studies are needed to identify enzymatic pathways catalysing isoprene metabolism and enable the accurate annotation of VOC metabolism from genomic signatures. Our findings extend previous work that has sought to explain the extraordinary success of the SAR11 clade and showed these cells evolved mechanisms that enable them to compete for some of the most labile forms of dissolved organic carbon in planktonic systems. The potential of heterotrophic bacteria to exert control on the emission of climate-active gasses is receiving increased attention because dynamic variation in the transmission of climate-active volatile compounds to the atmosphere is germane to our overall understanding of climate change and stability. Future work that dissects the biochemical mechanisms underlying VOC cycling will likely aim to mechanistically link marine microbial processes to trace gas emissions and atmospheric chemical transport models.

## Acknowledgements

This work was supported by the NASA North Atlantic Aerosols and Marine Ecosystems Study (NAAMES), award ID: NNX15AE70G, and the Simons Foundation International BIOS-SCOPE initiative (S.J.G.).

## References

Alvarez, L.A., Exton, D.A., Timmis, K.N., Suggett, D.J., and Mcgenity, T.J. (2009) Characterization of marine isoprene-degrading communities. *Environ Microbiol* **11**: 3280–3291.

Andreae, M.O., and Crutzen, P.J. (1997) Atmospheric aerosols: biogeochemical sources and role in atmospheric chemistry. *Science* **276**: 1052–1058.

Beale, R., Dixon, J.L., Arnold, S.R., Liss, P.S., and Nightingale, P.D. (2013) Methanol, acetaldehyde, and

acetone in the surface waters of the Atlantic Ocean. *J Geophys Res Ocean* **118**: 5412–5425.

Beale, R., Dixon, J.L., Smyth, T.J., and Nightingale, P.D. (2015) Annual study of oxygenated volatile organic compounds in UKshelf waters. *Mar Chem* **171**: 96–106.

Bonsang, B., Gros, V., Peeken, I., Yassaa, N., Bluhm, K., Zoellner, E., et al. (2010) Isoprene emission from phytoplankton monocultures: the relationship with chlorophyll-a, cell volume and carbon content. *Environ Chem* **7**: 554–563.

Booge, D., Schlundt, C., Bracher, A., Endres, S., and Zäncker, B. (2017) Marine isoprene production and consumption in the mixed layer of the surface ocean – a field study over 2 oceanic regions. *Biogeosci Discuss* **15**: 649–667.

Carini, P., Steindler, L., Beszteri, S., and Giovannoni, S.J. (2012) Nutrient requirements for growth of the extreme oligotroph ‘Candidatus *Pelagibacter ubique*’ HTCC1062 on a defined medium. *ISME J* **7**: 592–602.

Chen, Y.C., Peoples, O.P., and Walsh, C.T. (1988) *Acinetobacter* cyclohexanone monooxygenase: gene cloning and sequence determination. *J Bacteriol* **170**: 781–789.

Colomb, A., Yassaa, N., Williams, J., Peeken, I., and Lochte, K. (2008) Screening volatile organic compounds (VOCs) emissions from five marine phytoplankton species by head space gas chromatography/mass spectrometry (HS-GC/MS). *J Environ Monit* **10**: 325–330.

Davie-Martin C.L., Giovannoni S.J., Behrenfeld M.J., Penta W.B., Halsey K.H. (2020). Seasonal and spatial variability in the biogenic production and consumption of volatile organic compounds (VOCs) by marine plankton in the North Atlantic Ocean. *Front Mar Sci*, **7**. <http://doi.org/10.3389/fmars.2020.611870>

Dawson, R.A., Crombie, A.T., Pichon, P., Steinke, M., McGenity, T.J., and Murrell, J.C. (2021) The microbiology of isoprene cycling in aquatic ecosystems. *Aquat Microb Ecol* **87**: 79–98.

de Bruyn, W.J., Clark, C.D., Pagel, L., and Takehara, C. (2011) Photochemical production of formaldehyde, acetaldehyde and acetone from chromophoric dissolved organic matter in coastal waters. *J Photochem Photobiol A Chem* **226**: 16–22.

Dixon, J.L., Beale, R., and Nightingale, P.D. (2013) Production of methanol, acetaldehyde, and acetone in the Atlantic Ocean. *Geophys Res Lett* **40**: 4700–4705.

Dixon, J.L., Beale, R., Sargeant, S.L., Tarran, G.A., and Nightingale, P.D. (2014) Microbial acetone oxidation in coastal seawater. *Front Microbiol* **5**: 1–9.

Donoghue, N.A., and Trudgill, P.W. (1975) The metabolism of cyclohexanol by *Acinetobacter* NCIB 9871. *Eur J Biochem* **60**: 1–7.

Dress, A.W., Flamm, C., Fritsch, G., Grünwald, S., Kruspe, M., Prohaska, S.J., and Stadler, P.F. (2008) Noisy: identification of problematic columns in multiple sequence alignments. *Algorithms Mol Biol* **3**: 7.

EPA. (2016) On-line Tools for Site Assessment Calculation. URL <https://www3.epa.gov/ceampubl/learn2model/part-two/onsite/esthenry.html>.

Fischer, E.V., Jacob, D.J., Millet, D.B., Yantosca, R.M., and Mao, J. (2012) The role of the ocean in the global atmospheric budget of acetone. *Geophys Res Lett* **39**: n/a.

- Folkens, I., and Chatfield, R. (2000) Impact of acetone on ozone production and OH in the upper troposphere at high NO<sub>x</sub>. *J Geophys Res Atmos* **105**: 11585–11599.
- Fraaije, M.W., Wu, J., Heuts, D.P.H.M., Van Hellemond, E. W., Spelberg, J.H.L., and Janssen, D.B. (2005) Discovery of a thermostable Baeyer-Villiger monooxygenase by genome mining. *Appl Microbiol Biotechnol* **66**: 393–400.
- Giovannoni, S., Bibbs, L., Cho, J.C., Stapels, M., Desiderio, R., Vergin, K., *et al.* (2005a) Proteorhodopsin in the ubiquitous marine bacterium SAR11. *Nature* **438**: 82–85.
- Giovannoni, S., Tripp, J., Givan, S., Podar, M., Vergin, K., Baptista, D., *et al.* (2005b) Genome streamlining in a cosmopolitan oceanic bacterium. *Science* **309**: 1242–1245.
- Giovannoni, S.J. (2017) SAR11 bacteria: the most abundant plankton in the oceans. *Ann Rev Mar Sci* **9**: 231–255.
- Giovannoni, S.J., Halsey, K.H., Saw, J., Muslin, O., Suffridge, C.P., Sun, J., *et al.* (2019) A parasitic arsenic cycle that shuttles energy from phytoplankton to heterotrophic Bacterioplankton. *MBio* **10**: 10.
- González, J.M., and Moran, M.A. (1997) Numerical dominance of a group of marine bacteria in the  $\alpha$ -subclass of the class Proteobacteria in coastal seawater. *Appl Environ Microbiol* **63**: 4237–4242.
- Guenther, A.B., Jiang, X., Heald, C.L., Sakulyanontvittaya, T., Duhl, T., Emmons, L.K., and Wang, X. (2012) The model of emissions of gases and aerosols from nature version 2.1 (MEGAN2.1): an extended and updated framework for modeling biogenic emissions. *Geosci Model Dev* **5**: 1471–1492.
- Guillard, R.R.L., and Ryther, J.H. (1962) Studies of marine planktonic diatoms. I. *Cyclotella nana* Hustedt and *Detonula confervacea* Cleve. *Can J Microbiol* **8**: 229–239.
- Guindon, S., Dufayard, J.-F., Lefort, V., Anisimova, M., Hordijk, W., and Gascuel, O. (2010) New algorithms and methods to estimate maximum-likelihood phylogenies: assessing the performance of PhyML 3.0. *Syst Biol* **59**: 307–321.
- Hackenberg, S.C., Andrews, S.J., Airs, R., Arnold, S.R., Bouman, H.A., Brewin, R.J.W., *et al.* (2017) Potential controls of isoprene in the surface ocean. *Global Biogeochem Cycles* **31**: 644–662.
- Halsey, K.H., Carter, A.E., and Giovannoni, S.J. (2012) Synergistic metabolism of a broad range of C1 compounds in the marine methylotrophic bacterium HTCC2181. *Environ Microbiol* **14**: 630–640.
- Halsey, K.H., Giovannoni, S.J., Graus, M., Zhao, Y., Landry, Z., Thrash, J.C., *et al.* (2017) Biological cycling of volatile organic carbon by phytoplankton and bacterioplankton. *Limnol Oceanogr* **62**: 2650–2661.
- Hartmans, S., and de Bont, J.A.M. (1986) Acetol monooxygenase from *Mycobacterium* Py1 cleaves acetol into acetate and formaldehyde. *FEMS Microbiol* **36**: 155–158.
- Hausinger, R.P. (2007) New insights into acetone metabolism. *J Bacteriol* **189**: 671–673.
- Hense, I., Stemmler, I., and Sonntag, S. (2017) Ideas and perspectives: climate-relevant marine biologically driven mechanisms in earth system models. *Biogeosciences* **14**: 403–413.
- Johnston, A., Crombie, A.T., El Khawand, M., Sims, L., Whited, G.M., McGenity, T.J., and Colin Murrell, J. (2017) Identification and characterisation of isoprene-degrading bacteria in an estuarine environment. *Environ Microbiol* **19**: 3526–3537.
- Katoh, K., and Standley, D.M. (2013) MAFFT multiple sequence alignment software version 7: improvements in performance and usability. *Mol Biol Evol* **30**: 772–780.
- Kieber, R.J., Zhou, X., and Mopper, K. (1990) Formation of carbonyl compounds from UV-induced photodegradation of humic substances in natural waters: fate of riverine carbon in the sea. *Limnol Oceanogr* **35**: 1503–1515.
- Kotani, T., Yurimoto, H., Kato, N., and Sakai, Y. (2007) Novel acetone metabolism in a propane-utilizing bacterium, *Gordonia* sp. strain TY-5. *J Bacteriol* **189**: 886–893.
- Lemoine, F., Correia, D., Lefort, V., Doppelt-Azeroual, O., Mareuil, F., Cohen-Boulakia, S., and Gascuel, O. (2019) NGPhylogeny.fr: new generation phylogenetic services for non-specialists. *Nucleic Acids Res* **47**: W260–W265.
- Letunic, I., and Bork, P. (2019) Interactive tree of life (iTOL) v4: recent updates and new developments. *Nucleic Acids Res* **47**: W256–W259.
- Letunic, I., and Bork, P. (2021) Interactive tree of life (iTOL) v5: an online tool for phylogenetic tree display and annotation. *Nucleic Acids Res* **49**: W293–W296.
- Levine, S., and Krampitz, L.O. (1952) The oxidation of acetone by a soil diphtheroid. *J Bacteriol* **64**: 645–650.
- Liakakou, E., Vrekoussis, M., Bonsang, B., Donousis, C., Kanakidou, M., and Mihalopoulos, N. (2007) Isoprene above the eastern Mediterranean: seasonal variation and contribution to the oxidation capacity of the atmosphere. *Atmos Environ* **41**: 1002–1010.
- McGenity, T.J., Crombie, A.T., and Murrell, J.C. (2018) Microbial cycling of isoprene, the most abundantly produced biological volatile organic compound on earth. *ISME J* **12**: 931–941.
- Mckay, W.A., Turner, M.F., Jones, B.M.R., and Halliwell, C. M. (1996) Emissions of hydrocarbons from marine phytoplankton - some results from controlled laboratory experiments. *Atmos Environ* **30**: 2583–2593.
- Moore, E.R., Davie-Martin, C.L., Giovannoni, S.J., and Halsey, K.H. (2020) Pelagibacter metabolism of diatom-derived volatile organic compounds imposes an energetic tax on photosynthetic carbon fixation. *Environ Microbiol* **22**: 1720–1733.
- Mopper, K., Zhou, X., Kieber, R.J., Kieber, D.J., Sikorski, R. J., and Jones, R.D. (1991) Photochemical degradation of dissolved organic carbon and its impact on the oceanic carbon cycle. *Nature* **353**: 60–62.
- Morris, R.M., Frazar, C.D., and Carlson, C.A. (2012) Basin-scale patterns in the abundance of SAR11 subclades, marine Actinobacteria (OM1), members of the Roseobacter clade and OCS116 in the South Atlantic. *Environ Microbiol* **14**: 1133–1144.
- Morris, R.M., Rappé, M.S., Connon, S.A., Vergin, K.L., Siebold, W.A., Carlson, C.A., and Giovannoni, S.J. (2002) SAR11 clade dominates ocean surface bacterioplankton communities. *Nature* **420**: 806–810.
- Müller, J.F., and Brasseur, G. (1999) Sources of upper tropospheric HO<sub>x</sub>: a three-dimensional study. *J Geophys Res Atmos* **104**: 1705–1715.
- Pachiadaki, M.G., Brown, J.M., Brown, J., Bezuidt, O., Berube, P.M., Biller, S.J., *et al.* (2019) Charting the

- complexity of the marine microbiome through single-cell genomics. *Cell* **179**: 1623–1635.
- Palmer, P.I., and Shaw, S.L. (2005) Quantifying global marine isoprene fluxes using MODIS chlorophyll observations. *Geophys Res Lett* **32**: L0980.
- Patel, R.N., Hou, C.T., Laskin, A.I., and Felix, A. (1982) Microbial oxidation of hydrocarbons: properties of a soluble methane monooxygenase from a facultative methane-utilizing organism, *Methylobacterium* sp. strain CRL-26. *Appl Environ Microbiol* **44**: 1130–1137.
- Price, M.N., Dehal, P.S., and Arkin, A.P. (2010) FastTree 2 - approximately maximum-likelihood trees for large alignments. *PLoS One* **5**: 5.
- Rappé, M.S., and Giovannoni, S.J. (2003) The uncultured microbial majority. *Annu Rev Microbiol* **57**: 369–394.
- Sander, R. (2015) Compilation of Henry's law constants (version 4.0) for water as solvent. *Atmos Chem Phys* **15**: 4399–4981.
- Shaw, S.L., Chisholm, S.W., and Prinn, R.G. (2003) Isoprene production by *Prochlorococcus*, a marine cyanobacterium, and other phytoplankton. *Mar Chem* **80**: 227–245.
- Singh, H.B., O'Hara, D., Herlth, D., Sachse, W., Blake, D.R., Bradshaw, J.D., et al. (1994) Acetone in the atmosphere: distribution, sources, and sinks. *J Geophys Res* **99**: 1805.
- Sinha, V., Williams, J., Meyerhöfer, M., Riebesell, U., Paulino, A.I., and Larsen, A. (2007) Air-sea fluxes of methanol, acetone, acetaldehyde, isoprene and DMS from a Norwegian fjord following a phytoplankton bloom in a mesocosm experiment. *Atmos Chem Phys* **7**: 739–755.
- Sun, J., Steindler, L., Thrash, J.C., Halsey, K.H., Smith, D. P., Carter, A.E., et al. (2011) One carbon metabolism in SAR11 pelagic marine bacteria. *PLoS One* **6**: e23973.
- Taylor, D.G., Trudgill, P.W., Cripps, R.E., and Harris, P.R. (1980) The microbial metabolism of acetone. *J Gen Microbiol* **118**: 159–170.
- van Hylckama Vlieg, J.E.T., Leemhuis, H., Jeffrey, H., Spelberg, L., and Janssen, D.B. (2000) Characterization of the gene cluster involved in isoprene metabolism in *Rhodococcus* sp. Strain AD45. *J Bacteriol* **187**: 1956–1963.
- Villar, E., Vannier, T., Vernet, C., Lescot, M., Cuenca, M., Alexandre, A., et al. (2018) The ocean gene atlas: exploring the biogeography of plankton genes online. *Nucleic Acids Res* **46**: W289–W295.
- White, A., Giovannoni, S., Zhao, Y., Vergin, K., and Carlson, C. (2018) Elemental content and stoichiometry of SAR11 chemoheterotrophic marine bacteria. *Limnol Oceanogr (In Rev)* **4**: 44–51.
- Yang, J., and Zhang, Y. (2015) Protein structure and function prediction using I-TASSER. *Curr Protoc Bioinformatics* **52**: 5.8.1–5.8.15.
- Yang, M., Beale, R., Liss, P., Johnson, M., Blomquist, B., and Nightingale, P. (2014) Air-sea fluxes of oxygenated volatile organic compounds across the Atlantic Ocean. *Atmos Chem Phys* **14**: 7499–7517.
- Zhao, L., Chang, W., Xiao, Y., Liu, H., and Liu, P. (2013) Methylerythritol phosphate pathway of isoprenoid biosynthesis. *Annu Rev Biochem* **82**: 497–530.

### Supporting Information

Additional Supporting Information may be found in the online version of this article at the publisher's web-site:

**Fig. S1.** Maximum likelihood tree showing phylogenetic relationships of acetone/cyclohexanone monooxygenase protein sequences retrieved from TARA Oceans metatranscriptomes, shown in Fig. 3 in the main text. As expected, a large number of sequences recovered were taxonomically assigned by TARA to alphaproteobacteria. However, among the acetone/cyclohexanone monooxygenase homologues were many that formed distinct subclades assigned to other taxa. Although protein activities cannot be confidently assigned based on sequence similarities, this evidence suggests that a wide variety of marine bacteria might have the capacity to oxidize acetone.